THE JOURNAL OF BIOLOGICAL CHEMISTRY VOL. 288, NO. 25, pp. 17954–17967, June 21, 2013

Epithelial to Mesenchymal Transition Promotes Breast Cancer Progression via a Fibronectin-dependent STAT3 Signaling Pathway*

Received for publication, April 6, 2013, and in revised form, May 1, 2013 Published, JBC Papers in Press, May 7, 2013, DOI 10.1074/jbc.M113.475277

Nikolas Balanis[‡1], Michael K. Wendt[§1], Barbara J. Schiemann[§], Zhenghe Wang[§], William P. Schiemann[§2], and Cathleen R. Carlin[‡¶3]

From the [‡]Department of Physiology and Biophysics, the [§]Case Comprehensive Cancer Center, and [¶]Department of Molecular Biology and Microbiology, School of Medicine, Case Western Reserve University, Cleveland, Ohio 44106

Background: Cells perceive their environment through soluble growth factors and in response to extracellular matrix.
Results: STAT3 signaling can be activated by multiple pathways during breast cancer progression.
Conclusion: Fibronectin:STAT3 signaling promotes three-dimensional outgrowth of breast cancer cells.
Significance: This study demonstrates a novel mechanism by which STAT3 becomes activated by the extracellular matrix independent of the canonical EGF receptor signaling network.

We previously established that overexpression of the EGF receptor (EGFR) is sufficient to induce tumor formation by otherwise nontransformed mammary epithelial cells, and that the initiation of epithelial-mesenchymal transition (EMT) is capable of increasing the invasion and metastasis of these cells. Using this breast cancer (BC) model, we find that in addition to EGF, adhesion to fibronectin (FN) activates signal transducer and activator of transcription 3 (STAT3) through EGFR-dependent and -independent mechanisms. Importantly, EMT facilitated a signaling switch from SRC-dependent EGFR:STAT3 signaling in pre-EMT cells to EGFR-independent FN:JAK2:STAT3 signaling in their post-EMT counterparts, thereby sensitizing these cells to JAK2 inhibition. Accordingly, human metastatic BC cells that failed to activate STAT3 downstream of EGFR did display robust STAT3 activity upon adhesion to FN. Furthermore, FN enhanced outgrowth in three-dimensional organotypic cultures via a mechanism that is dependent upon β1 integrin, Janus kinase 2 (JAK2), and STAT3 but not EGFR. Collectively, our data demonstrate that matrix-initiated signaling is sufficient to drive STAT3 activation, a reaction that is facilitated by EMT during BC metastatic progression.

The extracellular matrix (ECM)[4] plays an integral role in the development and homeostatic maintenance of different organ systems (1). However, the signaling mechanisms that empower cancer cells to aberrantly utilize the ECM remain poorly defined (2). Recent evidence suggests that cooperation between integrins and growth factor receptors alters downstream signaling and may contribute to pathological responses of cancer cells to soluble ligands (3, 4). Indeed, we have shown that integrins form physical complexes with EGFR and TGF-β receptors giving rise to oncogenic signaling patterns and pathological responses to ligands (5–7).

High levels of EGFR expression within primary mammary tumors are strongly linked to the poor prognosis of human breast cancer (BC) (8, 9). Our previous studies indicate that EGFR is capable of transforming normal mammary epithelial cells (7). These findings and others (10) suggest that paracrine EGF signaling functions in concert with the process of epithelial mesenchymal transition (EMT) to facilitate tumor cell invasion and dissemination (7). Collectively, these studies have led to the clinical evaluation of EGFR inhibitors as potential targeted molecular therapies for BC (9, 11). Unfortunately, the results of these trials strongly indicate that targeted inhibition of EGFR does not offer any clinical benefit to BC patients (12). Consistent with this inherent resistance of BC to EGFR inhibition, we recently established that EGFR expression is actually diminished in the later stages of metastasis (13). Interestingly, metastatic breast carcinomas also display enhanced expression and altered distribution of fibronectin (FN) compared with normal breast (14). Along these lines, enhanced expression of FN is a well established marker of the EMT process (15), and survival analysis of BC patients with high levels of FN expression is predictive for an increased risk of mortality (14).

Signal transducer and activator of transcription 3 (STAT3) is a transcription factor that regulates cell proliferation and survival; it also functions as a major player that drives the growth of

* This work was supported, in whole or in part, by National Institutes of Health Grants GM081498 (to C. R. C.), CA129359 (to W. P. S.), CA166140 (to M. K. W.), and T32 HL007653 (to N. B.), and pilot project Grant CA043703 from development funds of the Case Comprehensive Cancer Center Support (to C. R. C. and Z. W.).
[1] Both authors contributed equally to this work.
[2] To whom correspondence may be addressed: Wolstein Research Building, Case Western Reserve University, 2103 Cornell Rd., Cleveland, OH 44106. Tel.: 216-368-5763; Fax: 216-369-1166; E-mail: william.schiemann@case.edu.
[3] To whom correspondence may be addressed: Dept. of Molecular Biology and Microbiology, School of Medicine, Case Western Reserve University, 10900 Euclid Ave., Cleveland, OH 44106. Tel.: 216-368-8939; Fax: 216-368-3055; E-mail: cathleen.carlin@case.edu.
[4] The abbreviations used are: ECM, extracellular matrix; BC, breast cancer; EGFR, epidermal growth factor receptor; EMT, epithelial to mesenchymal transition; FN, fibronectin; HER2, human epidermal growth factor receptor 2; JAK2, Janus kinase 2; NMuMG, normal mouse mammary gland; STAT3, signal and activator of transcription 3; TNBC, triple-negative breast cancer; WT, wild-type.

stem-like BC cells (16, 17). STAT3 can be activated by several signaling systems including those stimulated by interleukin-6 (IL-6) (18), Oncostatin M (19), interferons (20), and EGF (21). In light of our recent study that demonstrated the ability of the matrix to directly activate EGFR (5), we hypothesized that FN:EGFR signaling could play a pivotal role in the activation of STAT3 during BC progression.

We show herein that FN is readily capable of activating STAT3 in the absence of any soluble ligands, a reaction that is markedly increased in metastatic BC cells. Mechanistically, we demonstrate that EMT leads to pathway switching of STAT3 activation, such that nonmetastatic BC cells employ a SRC-dependent EGF:EGFR axis to stimulate STAT3, whereas their metastatic counterparts switch to a FN:β1 integrin:FAK/PYK2:JAK2 axis to stimulate STAT3. Importantly, interdiction of FN:STAT3 signaling, but not that of EGFR:STAT3, readily prevents the three-dimensional outgrowth of metastatic BC cells in a pulmonary organotypic culture system. In summary, our data suggest a mechanism by which metastatic BC cells exploit EMT to circumvent growth factor signaling, and directly engage the ECM to activate critical downstream signaling pathways.

EXPERIMENTAL PROCEDURES

Cell Lines, Cell Culture, and Reagents—Normal mouse mammary gland (NMuMG) epithelial cells and human MDA-MB-231 and MDA-MB-468 BC cells were purchased from ATCC (Manassas, VA) and cultured as described previously (7, 22, 23). Mouse NR6 fibroblasts are an NIH-3T3 variant lacking endogenous EGFR expression (24). Construction of NMuMG and NR6 cell lines expressing human WT-EGFR or EGFR with 679,680-LL converted to AA (EGFR-AA) were described previously (5, 25). Cells were maintained at 37 °C in a humidified atmosphere of 5% CO_2 and 95% air in Dulbecco's modified Eagle's medium (DMEM) supplemented with 10% fetal bovine serum (FBS). Cell lines expressing recombinant proteins were selected and maintained in media supplemented with the appropriate antibiotic (G418 (MP Biomedicals, Solon, OH) or puromycin (Invitrogen)). NMuMG cells were stimulated with TGF-β1 (5 ng/ml) to induce EMT as described previously (13). The human MCF10A parental cell line and its increasingly tumorigenic variants T1k and Ca1h were cultured according to published methods (26). Pharmacological inhibitors were as follows: AG1478, target: EGFR (Cayman Pharmaceuticals); Erlotinib, target: EGFR (Cayman Pharmaceuticals); PF573228, target: FAK (Pfizer Inc.); PF562271, target: FAK/PYK2 (Pfizer Inc.); WP1066, target: JAK2 (EMD Millipore); Stattic, target: STAT3 (EMD Millipore); STAT3 inhibitor VII, target: upstream activators of STAT3 (EMD Millipore).

Cell Harvesting and Immunoblotting—Cells were washed 3 times with PBS supplemented with 5 mM EDTA, 5 mM EGTA, and a phosphatase inhibitor mixture (10 mM NaF, 10 mM $Na_4P_2O_7$, and 1 mM Na_3VO_4). Cells were lysed with 1% Nonidet P-40 in a solution of 50 mM Tris-HCl, pH 7.4, supplemented with 150 mM NaCl, the phosphatase inhibitor mixture, and a protease inhibitor mixture (100 μM phenylmethylsulfonyl fluoride, 10 μg/ml of aprotinin, 10 μg/ml of leupeptin, 4 μg/ml of pepstatin). Cell lysates were clarified by high-speed centrifugation and protein concentrations were determined by Bradford assay (Bio-Rad). Equal aliquots of total cellular protein were resolved by SDS-PAGE and transferred to nitrocellulose filters for immunoblotting using standard methods. Antibody concentrations and suppliers are as follows: Cell Signaling Technologies, EGFR(Tyr-845), 1:1000, number 2231; EGFR(Tyr-992), 1:1000, number 2235; EGFR(Tyr-1086), 1:1000, number 2220; EGFR, 1:1000, number 4267; β3 Integrin, 1:1000, number 4702; β1 Integrin, 1:2000, number 4706; pErk1/2, 1:2000, number 4377; Erk1/2, 1:1000, number 9102; pSTAT3, 1:1000, number 9145; STAT3, 1:1000, number 9132; pSMAD2, 1:1000, number 3108; and SMAD2/3; 1:1000, number 8685; Harlan Laboratories, EGFR1, 1:50 FACS, custom; BD Bioscience, E-Cadherin, 1:5000, number 610181; BD Pharmingen, β1 Integrin Neutralizing, 10 μg/ml, number 562219 and fibronectin, 1:5000, number 610077, Santa Cruz Biotechnologies, β-actin, 1:1000, sc47778; and Sigma, β-actin, 1:2500, number A5441.

Cell Morphometry Measurements—Cells were permeabilized with 0.5% β-escin in a solution of 80 mM PIPES, pH 6.8, supplemented with 5 mM EGTA and 1 mM $MgCl_2$ for 5 min and fixed with 3% paraformaldehyde/PBS for 15 min as described previously (27). Cells were stained with rhodamine-conjugated phalloidin and confocal images were acquired with a Zeiss LSM 510 Meta laser scanning microscope (Carl Zeiss MicroImaging, Jenna, Germany) using a ×40 Plan Apo NA 1.4 objective and Zeiss LSM software (Carl Zeiss MicroImaging, Jenna, Germany). Filopodia were counted using MetaMorph software (Molecular Devices, Sunnydale, CA). Briefly, individual cells were filtered by determining threshold values for average pixel intensity. The number of filopodia per cell was determined by counting only filopodia with fluorescent intensity above the average intensity following thresholding that crossed the cell edge and were ≥2 μm. Cell shapes were determined by computing shape factor parameters, which measure cell area as a function of cell perimeter (equation $4A\pi/P^2$, where A is the cell area and P is the perimeter) as described previously (5, 28). This value varies from 0 to 1 for elongated to more rounded shapes, respectively (29).

Cell Biological Assays—For cell adhesion experiments, cells grown to 80% confluence were serum-starved for 5 h in media supplemented with 0.5% bovine serum albumin (BSA). NMuMG cell populations were serum-starved in DMEM that was also supplemented with insulin (10 μg/ml) and if applicable TGF-β1 (5 ng/ml). Cells were detached from tissue culture plastic with 0.25% trypsin/EDTA, which was inactivated with a 2-fold volume of serum-free media supplemented with soybean trypsin inhibitor (0.5 mg/ml; Invitrogen). Cells were allowed to adhere to polystyrene dishes or glass coverslips coated with ECM proteins (10 μg/ml) at a density of 4×10^4 cells/mm surface area. Control cells were kept in suspension in polystyrene dishes coated with BSA (10 mg/ml). DNA synthesis was measured by [^{3}H]thymidine incorporation as previously described (26). Cell fractionation was performed using a Nuclear/Cytosol Fractionation Kit (Biovision, Milpitas, CA) according to the manufacturers' instructions.

Three-dimensional Organotypic Growth Assays—Ninety-six-well plates were coated with Cultrex (50 μl/well; Trevigen Inc.,

Gaithersburg, MD) and cells were resuspended in DMEM supplemented with 10% FBS and 4% Cultrex (150 μl/well). To assess FN-specific growth effects, 96-well plates were similarly coated with Cultrex or a 2:1 mixture of Cultrex:FN using a 1 mg/ml of FN stock. Luciferase expressing MDA-MB-231 or NMuMG-EGFR cells were resuspended in DMEM supplemented with 2% FBS and 2% Cultrex, or with a 2% solution of a 1:3 Cultrex/FN mixture. Cells were seeded at a density of 1×10^3 cells/well. Media was replaced every 4 days and organoid outgrowth was detected by adding D-luciferin potassium salt (Caliper Life Sciences, Hopkinton, MA) to induce bioluminescence, which was quantified using a GloMax-Multi detection system (Promega, Madison, WI). Longitudinal cell growth was normalized to an initial reading taken 30 min after seeding as a baseline. Organotypic cultures were also examined by phase-contrast microscopy to assess their morphology.

Tumor Growth—NMuMG cell lines were resuspended in sterile PBS supplemented with 5% Matrigel (2×10^6 cells/50 μl) and subsequently injected directly into the nipple of 6-week-old female nu/nu mice (Charles River, Wilmington, MA) to allow seeding within the mammary ducts. Tumor growth was monitored by digital caliper measurements at the indicated time points using the following equation: volume = $(\text{length}^2) \times (\text{width}) \times (0.5)$.

In Silico Analyses—The Cancer Cell Line Encyclopedia contains a repository of $\log_2$ expression data derived from Affymetrix U133A + 2.0 Arrays for 947 unique human cancer cell lines. Human BC cell lines were annotated based on literature search for their basal *versus* luminal BC status (30, 31). Expression data for FN was extracted for each cell line using a robust microarray algorithm and reconverted from a $\log_2$ to a linear scale as described in Ref. 32.

GEO Dataset GSE36953 contains expression data using the Affymetrix U133A + 2.0 for MDA-MB-231 cells under various culture conditions. The dataset contained MAS5.0 normalized expression data, which was used to determine fold-changes between groups. Fold-change in transcript expression was determined by comparing the levels observed in MDA-MB-231 tumors *versus* those measured in their respective two-dimensional cultured counterparts.

Kaplan-Meier Plots—The Kaplan-Meier plot is an on-line biomarker validation tool that compares the proportional survival of patient groups based on relative biomarker expression using microarray data. This tool was employed to estimate survival probabilities for BC patients split into two groups based on FN gene expression. This analysis was carried out by extracting microarray data for 2878 BC patients and overall survival data for 1027 patients from a database described in Ref. 33 using the sole_at probe (214702_at).

Statistical Analyses—Statistical analyses were carried out using an unpaired Student's *t* test where p values < 0.05 were considered statistically significant.

RESULTS

FN Activates an EGFR:STAT3 Signaling Axis—We previously established that FN and EGFR form a signaling complex coupled to the activation of the RhoA antagonist p190RhoGAP in newly adherent cells (5). However, the extent to which FN:EGFR cross-talk induces other signaling pathways remains unexplored. To address this question, we engineered NR6 cells, which lack endogenous EGFR expression to stably express equivalent levels of either wild-type EGFR (WT-EGFR) or an EGFR mutant with a dialanine substitution for Leu-679 and Leu-680 (EGFR-AA) (5, 34, 35). Importantly, the EGFR-AA mutant is defective for Tyr-845 phosphorylation by SRC, an event that is necessary for STAT3 activation (36). Accordingly, EGF stimulation of WT-EGFR expressing cells elicited robust phosphorylation of EGFR at Tyr-845 and a STAT3 reaction that failed to occur in EGFR-AA expressing cells (Fig. 1*A*). Importantly, adhesion to FN induced the phosphorylation of Tyr-845 in cells expressing WT-EGFR, but not in those expressing EGFR-AA (Fig. 1*B*). Furthermore FN-mediated Tyr-845 phosphorylation of EGFR was dependent on the kinase activities of EGFR and SRC and was not triggered by the alternative ECM protein laminin (Fig. 1*C*). Along these lines, EGFR expression was specifically required for FN-induced activation of STAT3, which contrasts with that of Erk1/2 that was similarly stimulated in control and EGFR expressing cells (Fig. 1*D*). Similar to ligand-mediated activation of STAT3, FN-mediated STAT3 signaling was sensitive to EGFR and SRC kinase inhibitors (Fig. 1*E*). Consistent with its activation and role as a transcription factor, phosphorylated STAT3 underwent nuclear translocation in response to FN exposure, opening the possibility of unique FN-induced STAT3 gene expression profiles (Fig. 1*F*). In addition to its nuclear function, cytoplasmic STAT3 also plays a role in regulation of cytoskeleton (37). Accordingly, FN-induced formation of filopodial membrane protrusions was potently blocked by treating NR6-EGFR cells with Stattic, an inhibitor of STAT3 dimerization (38) (Fig. 1, *G* and *H*). Collectively, these findings show that FN is capable of activating the STAT3 signaling system independent of ligand stimulation.

STAT3 Activation Is Critical for EGFR-mediated Transformation of Mammary Epithelial Cells—We recently established that NMuMG cells are transformed by overexpression of EGFR (hereafter referred as NME cells) (7). Interestingly, we show here that overexpression of EGFR-AA failed to transform NMuMG cells (hereafter referred to as NME-AA cells; Fig. 2, *A–D*). Consistent with these *in vivo* findings, parental and NME-AA cells formed small differentiated acinar structures when propagated in three-dimensional organotypic cultures (Fig. 2*E*). In stark contrast, NME cells produced much larger filled organoids that are characteristic of transformed cells (39) (Fig. 2*E*). This aberrant growth in three-dimensional culture was normalized by administration of the EGFR kinase inhibitors AG1478 and Erlotinib, as well as by that of two different STAT3 inhibitors, (i) Inhibitor VII, which targets STAT3 pathway members, and (ii) Stattic, which blocks STAT3 dimerization and activation. In contrast, the aberrant growth of the NME cells was not affected by WP1006 (Fig. 2*F*), which inhibits JAK2-mediated activation of STAT3.

Unlike NR6 fibroblasts (Fig. 1*D*), the parental NMuMG cells express endogenous EGFR and readily activate Erk1/2 and Akt in response to EGF (Fig. 2, *G* and *H*) (13). However, only NME cells displayed robust STAT3 phosphorylation when stimulated with EGF (Fig. 2, *G* and *H*). Moreover, EGF-stimulated STAT3 activation was dependent on SRC kinase, whereas

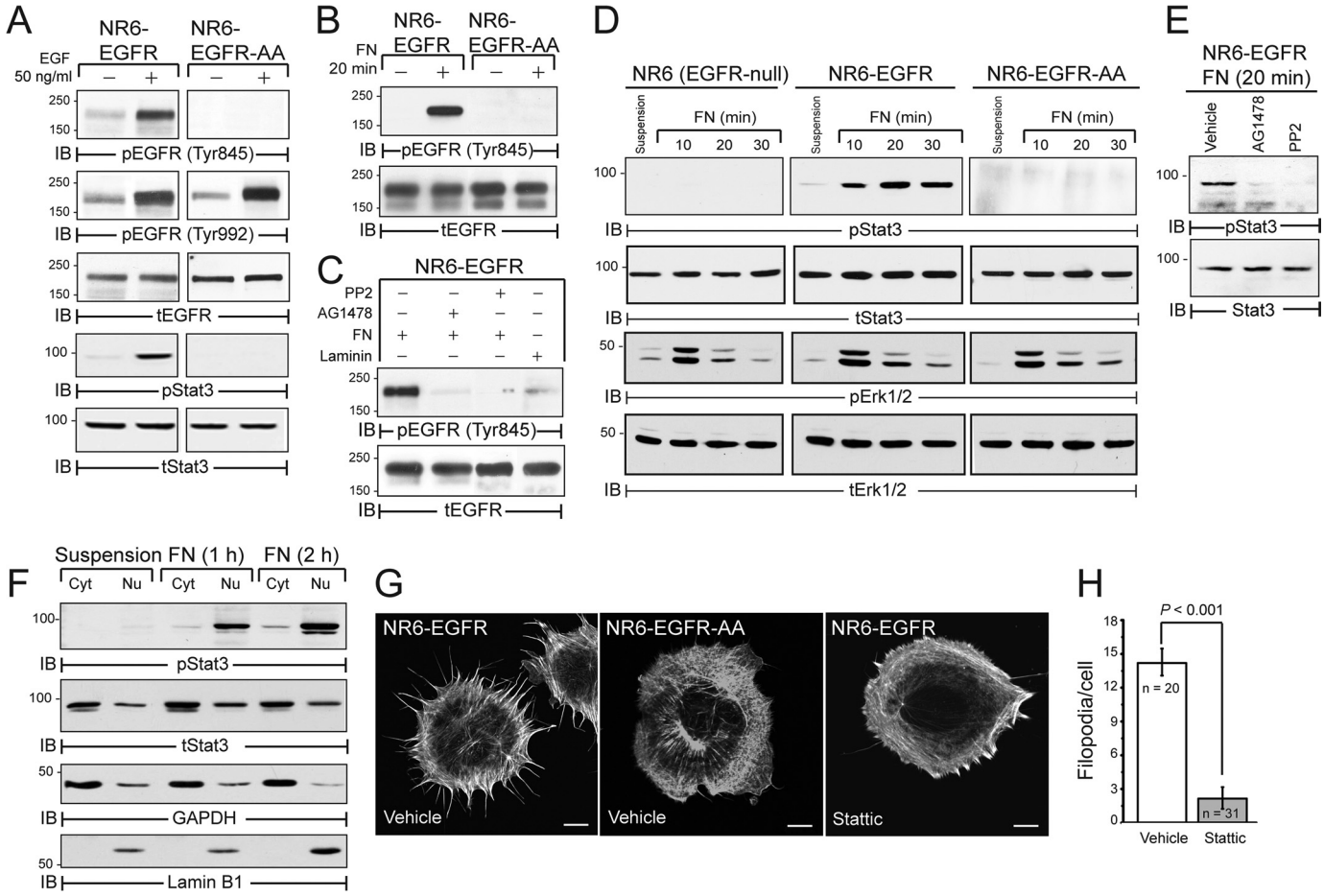

FIGURE 1. **EGFR-dependent STAT3 signaling in a heterologous reconstitution system.** *A*, EGFR-null NR6 cells reconstituted with wild-type human EGFR (*NR6-EGFR*) or EGFR with a 679-LL dialanine substitution (*NR6-EGFR-AA*) were harvested under basal conditions (−) or following a 30-min EGF stimulation (+). Equal protein aliquots were immunoblotted with phospho-specific and total EGFR and STAT3 antibodies. *B*, NR6-EGFR or NR6-EGFR-AA cells were left in suspension (−) or adhered to FN for 20 min (+). Equal protein aliquots were immunoblotted with phospho-specific and total EGFR antibodies. *C*, NR6-EGFR cells pretreated with vehicle, EGFR (1 μM AG1478), or SRC (10 μM PP2) kinase-specific inhibitors and subsequently adhered to FN as in *panel A* or laminin. Equal protein aliquots were immunoblotted with phospho-specific and total EGFR antibodies. *D*, parental and EGFR-expressing NR6 cells were adhered to FN for the indicated amounts of time and equal protein aliquots were immunoblotted with phospho-specific (*p*) and total (*t*) STAT3 and Erk1/2 antibodies. *E*, NR6-EGFR cells were pretreated with the indicated kinase inhibitors and subsequently adhered to FN. Equal protein aliquots were analyzed by immunoblotting with phospho-specific and total protein antibodies for STAT3. *F*, NR6-EGFR cells were kept in suspension or adhered to FN for the indicated amounts. Cells were subjected to cell fractionation prior to immunoblotting with phospho-specific and total STAT3 antibodies. Cytosolic (*Cyt*) and nuclear (*Nu*) fractions were confirmed by immunoblot for GAPDH and Lamin B1, respectively. *G*, representative confocal images of NR6-EGFR cells adhered to FN for 20 min in the presence of vehicle or the STAT3 inhibitor Stattic (5 μM) and then stained with phalloidin to visualize the actin cytoskeleton. *H*, data for NR6-EGFR cells in *G* quantified as described under "Experimental Procedures." Data are the mean number of filopodia per cell ≥2 mm in length/cell ± S.E.

Erk1/2 activation was not (Fig. 2*H*). Collectively, these data establish that STAT3 is aberrantly activated downstream of Src-dependent EGFR signaling, and suggest that this pathway likely plays a critical role in the transformed phenotype of mammary epithelial cells that overexpress this growth factor receptor.

Autocrine Expression of FN Is Associated with Aberrant STAT3 Phosphorylation—To further examine the potential role of STAT3 in BC progression, we analyzed the HRAS-driven human MCF10A BC progression series, consisting of normal (10A), indolent (T24-HRAS-transformed T1K), and malignant (Ca1h) cell lines (40). Fig. 3*A* shows that malignant Calh cells acquire a mesenchymal phenotype characterized by down-regulation of E-cadherin and up-regulation of FN and β1 integrin as compared with their nonmalignant counterparts. Furthermore, autocrine FN expression in Ca1h cells was highly correlated with constitutive STAT3 activation by an EGFR-independent mechanism (Fig. 3, *A* and *B*). These findings suggest that EMT-mediated up-regulation of FN and β1 integrin may facilitate the activation of STAT3 in more aggressive BC.

EMT Selectively Drives a Pathway Switch Upstream of STAT3 Activation—To further examine the role of EMT in EGFR:STAT3 and FN:STAT3 signaling we utilized TGF-β1 to induce a mesenchymal state in the NME cells, a measure we previously observed to be capable of increasing the invasion and metastasis of these cells (7). IL-6 stimulation of STAT3 was unaffected by induction of EMT (Fig. 4*A*). In contrast, short (6 h, 48 h) or long (4 weeks) term exposure of NME cells to TGF-β1 prior to EGF stimulation led to a dramatic reduction in the ability of these cells to activate STAT3 via this pathway (Fig. 4, *B*–*D*). Furthermore, *ex vivo* NME cells harvested from "post-EMT" tumors selectively displayed reduced EGF-mediated STAT3 signaling as compared with their pre-EMT counterparts despite the fact that ligand-induced Erk1/2 activation was

maintained in both cell populations (Fig. 4*E*). In sharp contrast, TGF-β1-induced EMT potently enhanced the ability of FN to activate STAT3 (Fig. 5*A*). Importantly, EGFR and Src inhibitors that abrogated FN:STAT3 signaling in pre-EMT cells had essentially no effect on FN:STAT3 signaling in their post-EMT counterparts (Fig. 5*B*). Similar to Fig. 4*E*, the activation of

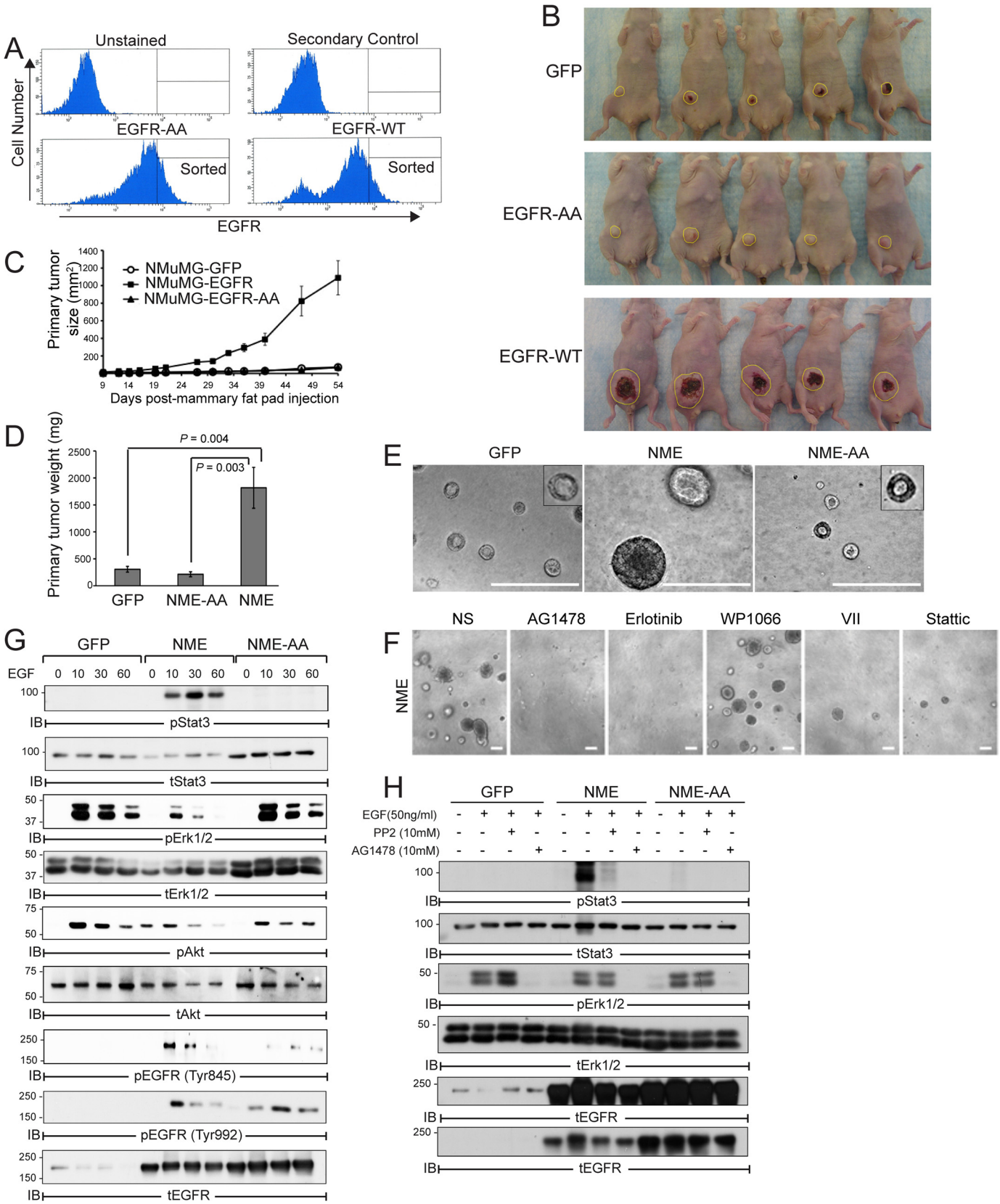

Erk1/2 by FN was unaffected by the EMT status of the cells (Fig. 5*A*), and was similarly impaired by EGFR kinase inhibition in both cell populations (Fig. 5*B*). Concomitant with this enhanced response to FN, STAT3 phosphorylation switched from a pathway regulated by Src and EGFR (Fig. 5*B*) to one dependent upon JAK2 (Fig. 5*C*). Importantly, this pathway switching sensitized post-EMT NME cells to pharmacologic inhibition of JAK2 (Fig. 5, *D* and *E*). Taken together, these data strongly suggest that EMT programs mediate a pathway switch in STAT3 activation away from EGFR-dependent signaling in pre-EMT cells to an EGFR-independent pathway regulated by FN and JAK2 during EMT and the metastatic progression of BCs.

FN Facilitates STAT3 Signaling in Metastatic BC Cells Independent of EGFR—Thus far we have shown that FN is capable of activating STAT3 independent of EGFR following induction of EMT (Fig. 5, *A* and *B*). Therefore, we hypothesized that FN adhesion maintains STAT3 signaling independent of growth factor receptor signaling during metastatic outgrowth. This hypothesis was tested in human MDA-MB-231 BC cells, which were originally derived from a pleural effusion of a metastatic BC patient (41). Interestingly, Src-dependent EGFR signaling failed to elicit STAT3 phosphorylation in MDA-MB-231 cells as compared with the MDA-MB-468 cells, in which EGFR is genomically amplified and therefore highly expressed (Fig. 6*A*) (42, 43). In contrast, IL-6 activated STAT3 via a JAK2-dependent manner in the MDA-MB-231 cells (Fig. 6*B*). Consistent with the lack of EGFR:STAT3 signaling, FN adhesion elicited robust STAT3 phosphorylation in MDA-MB-231 cells (Fig. 6*C*) by a mechanism that was independent of EGFR and Src kinase activity (Fig. 6*D*). Treatment of the MDA-MB-231 cells with TGF-β1 can enhance their pulmonary metastasis (44). Along these lines, treatment of MDA-MB-231 cells with TGF-β1 led to potent induction of β1 integrin and FN expression (Fig. 6*E*). Interestingly, gene microarray data from *in vitro* basal-like BC cell lines, including MDA-MB-231 cells, exhibit high levels of FN expression as compared with luminal BC (Fig. 6*F*). Furthermore, expression of FN is enhanced in MDA-MB-231 primary tumor xenografts *versus in vitro* cultured cells (Fig. 6*G*). Thus, enhanced autocrine FN expression by cells at the primary tumor may provide a local oncogenic niche that not only maintains STAT3 signaling independent of other extracellular factors, but also enhances STAT3 signaling in surrounding cells. Accordingly, we found that high FN expression in the primary tumor was linked to poor overall survival in a cohort of 1027 BC patients (Fig. 6*H*) (33).

FN:STAT3 Signaling Is Regulated by a Focal Adhesion Kinase-dependent:JAK2 Pathway in MDA-MB-231 Cells—We next sought to elucidate the mechanism whereby FN activates STAT3 independent of EGFR. Integrins are transmembrane receptors that sense the ECM and are linked to intracellular signaling modules via the focal adhesion complex (45). Indeed, we previously established that several integrins and focal adhesion complex proteins are up-regulated during TGF-β-induced EMT (6, 22, 26). These findings raise the possibility that an integrin-mediated axis could facilitate FN:STAT3 signaling during EMT and metastasis. Accordingly, adhesion to FN elicited robust activation of two related focal adhesion kinases, FAK and PYK2, as well as that of JAK2 (Fig. 7*A*). FN-induced STAT3 activation was blocked by treating cells with small molecule inhibitor PF-573228 (PF228) that specifically targets FAK (Fig. 7*B*). Use of a related compound, PF-562271 (PF271), which targets both FAK and PYK2, was more effective at lower concentrations than PF228, suggesting a preferential role for PYK2 in mediating FN:STAT3 signaling in the MDA-MB-231 metastatic BC cell line (Fig. 7*B*). Moreover, FN-mediated JAK2 phosphorylation was also dependent on FAK/PYK2, but independent of EGFR kinase activity (Fig. 7*C*). Similar to post-EMT NME cells (Fig. 5*E*), FN-induced STAT3 activation was also blocked by the JAK2 inhibitor WP1066 in MDA-MB-231 cells (Fig. 7*D*).

Consistent with a potential role for acute STAT3 activation in modulating the cytoskeleton (Fig. 1), administration of JAK2 (WP1066) or STAT3 (Stattic) inhibitors prevented MDA-MB-231 cells from acquiring an elongated mesenchymal morphology when cultured on FN (Fig. 7, *E* and *F*). In contrast, targeting EGFR kinase activity under these same conditions had little to no effect on cell morphology (Fig. 7, *E* and *F*). Collectively, these findings have delineated a novel FN:FAK/PYK2:JAK2 signaling axis that drives the sustained activation of STAT3 in metastatic BC cells.

The FN:STAT3 Signaling Axis Regulates Three-dimensional Outgrowth of Metastatic BC Cells—We (13, 22) and others have previously established the importance of cytoskeletal dynamics (46) and β1 integrin (2, 47) in regulating the metastatic outgrowth of BC. Therefore, we next sought to identify the impact of inactivating FN:STAT3 signaling in preventing three-dimensional outgrowth. Using a three-dimensional organotypic culture system to recapitulate the compliance of the pulmonary microenvironment, we found that the outgrowth of MDA-MB-231 cells was significantly enhanced by FN supplementation (Fig. 8, *A* and *B*). Moreover, supplemental FN enabled MDA-

FIGURE 2. **STAT3 activation is required for EGFR-dependent transformation of NMuMG cells.** *A,* NMuMG cells were stably transfected to express either wild-type human EGFR (*EGFR-WT*) or a 679-LL dialanine substitution (*EGFR-AA*), whose cell surface expression in stable polyclonal NMuMG cell populations was verified flow cytometry and cells were sorted for equivalently elevated levels of EGFR in indicated (denoted as *sorted*). *B,* control (GFP), EGFR-WT (*NME*), or EGFR-AA (*NME-AA*) expressing NMuMG cells (2×10^6) isolated in *panel A* were engrafted onto the mammary fat pad of female *nu/nu* mice. Shown are all mice from each group 54 days after fat pad inoculation (*yellow line* denotes outline of mammary lesions). *C* and *D*, control NMuMG cells (2×10^6) expressing GFP, WT-EGFR (*NME*), or EGFR-AA (*NME-AA*) were injected into mammary fat pads of female *nu/nu* mice. Mean tumor size over a 54-day period (*C*) and mean tumor weight at day 54 (*D*). Data are mean $\pm$ S.E. of 5 mice per group. *E*, representative photomicrographs of cells propagated in three-dimensional organotypic culture for 10 days. *Bar*, $\times$200 magnification. *Insets*, high magnification images of hollowed acinar structures formed by control and NME-AA cells. *F*, representative photomicrographs of NME propagated in three-dimensional cultures in the absence (*NS*) or presence of the indicated inhibitors (1 μM each) for 10 days. *Bar*, $\times$100 magnification. *C* and *D*, representative data from at least three independent experiments. *G*, NMuMG-derived cells were stimulated with EGF up to 30 min. *H*, NMuMG cells were pretreated with SRC (10 μM PP2) or EGFR (1 μM AG1478) kinase-specific inhibitors 2 h prior to EGF stimulation. *G* and *H*, equal protein aliquots were analyzed by immunoblotting with the indicated antibodies.

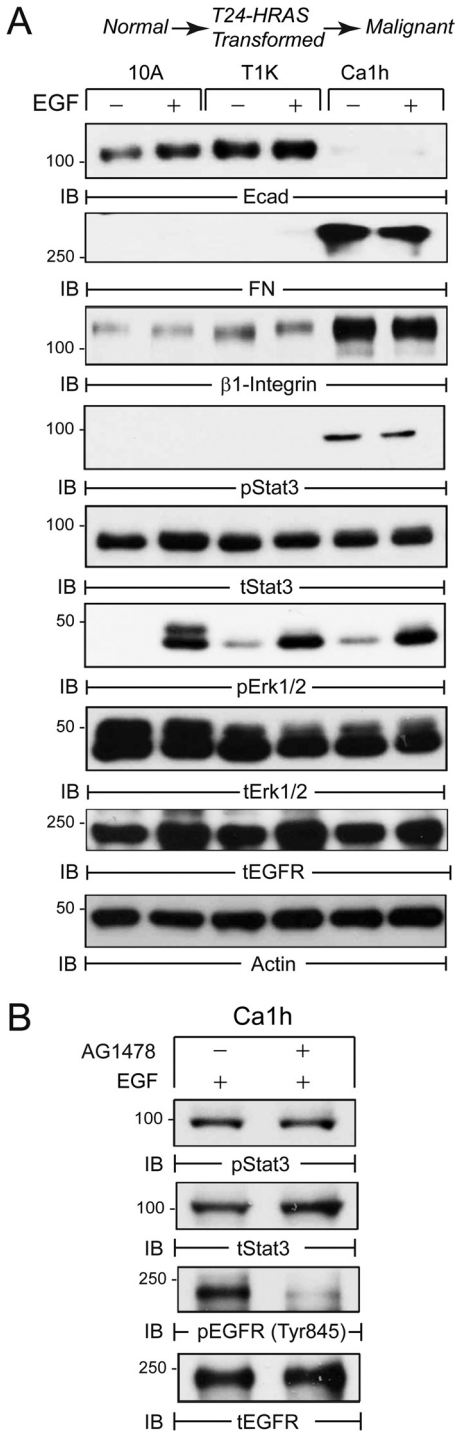

FIGURE 3. **Autocrine FN production correlates with STAT3 activation in a human BC progression model.** *A*, human MCF10A (10A) cells and tumorigenic variants T1k and Ca1h serum deprived for 24 h and subsequently stimulated with EGF for 30 min. Equal protein aliquots were analyzed by immunoblot (*IB*) with the indicated phospho (*p*) and total (*t*) antibodies. *B*, malignant Ca1h cells were treated with the EGFR inhibitor (1 μM AG1478) and analyzed by immunoblot with phospho-specific and total EGFR and STAT3 antibodies. Data are representative of at least two independent experiments.

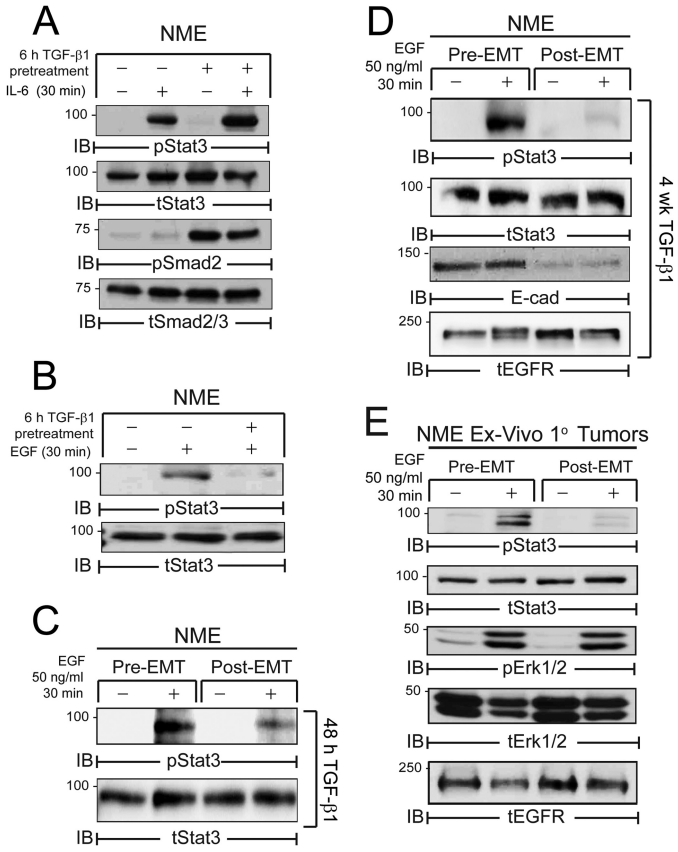

FIGURE 4. **EMT inhibits EGFR-dependent STAT3 signaling.** *A*, NME cells were serum deprived for 6 h in the presence or absence of TGF-β1 (5 ng/ml) and subsequently stimulated with IL-6 (50 ng/ml) for 30 min. *B*, NME cells were serum deprived in the presence or absence of TGF-β1 as in *panel A* and subsequently stimulated with EGF (50 ng/ml) for 30 min. *C* and *D*, NME cells were cultured in the presence of TGF-β1 for 48 h (*C*) or 4 weeks (*D*), to elicit an EMT. These pre- and post-EMT cell populations serum were deprived for 6 h and stimulated with EGF as in *panel B*. *E*, NME cells were cultured *ex vivo* from mammary fat pad tumors generated by pre- and post-EMT cell populations. These cells were then serum deprived and treated with EGF as in *panel B*. *A–E*, equal protein aliquots were analyzed by immunoblotting (*IB*) with the indicated antibodies and data are representative of at least two independent experiments.

MB-231 cells to transition from branched morphologies to cell-dense three-dimensional structures (Fig. 8*A*), a phenotype that we previously linked to enhanced metastatic capacities of BC cells (7, 13). Underscoring the importance of β1 integrin in mediating these events, we found that administration of neutralizing β1 integrin antibodies prevented FN-induced three-dimensional outgrowth as compared with an isotype control antibody (Fig. 8*C*). In contrast, MDA-MB-231 cells were resistant to EGFR kinase inhibition in the presence of supplemental FN (Fig. 8, *A* and *D*). Pharmacological inhibition of STAT3 using two mechanistically distinct compounds (STAT3 inhibitor VII and Stattic) completely abrogated three-dimensional outgrowth of MDA-MB-231 cells (Fig. 8, *A* and *D*). In contrast to NME cells, which are nonmetastatic (Fig. 4*H*), outgrowth of MDA-MB-231 cells was also blocked by administration of WP1066 to inhibit JAK2 (Fig. 8, *A* and *D*). Collectively, these data establish a role for a FN:STAT3 signaling module in driving the three-dimensional outgrowth of metastatic BC. Furthermore, our data demonstrate a role for β1 integrin in a complementary STAT3 pathway that employs FN linked to a JAK2:STAT3 signaling network in place of EGFR in late-stage BC.

DISCUSSION

BC can be divided into several genetically distinct subgroups. Clinically, those BCs belonging to the "triple negative" (TNBC)

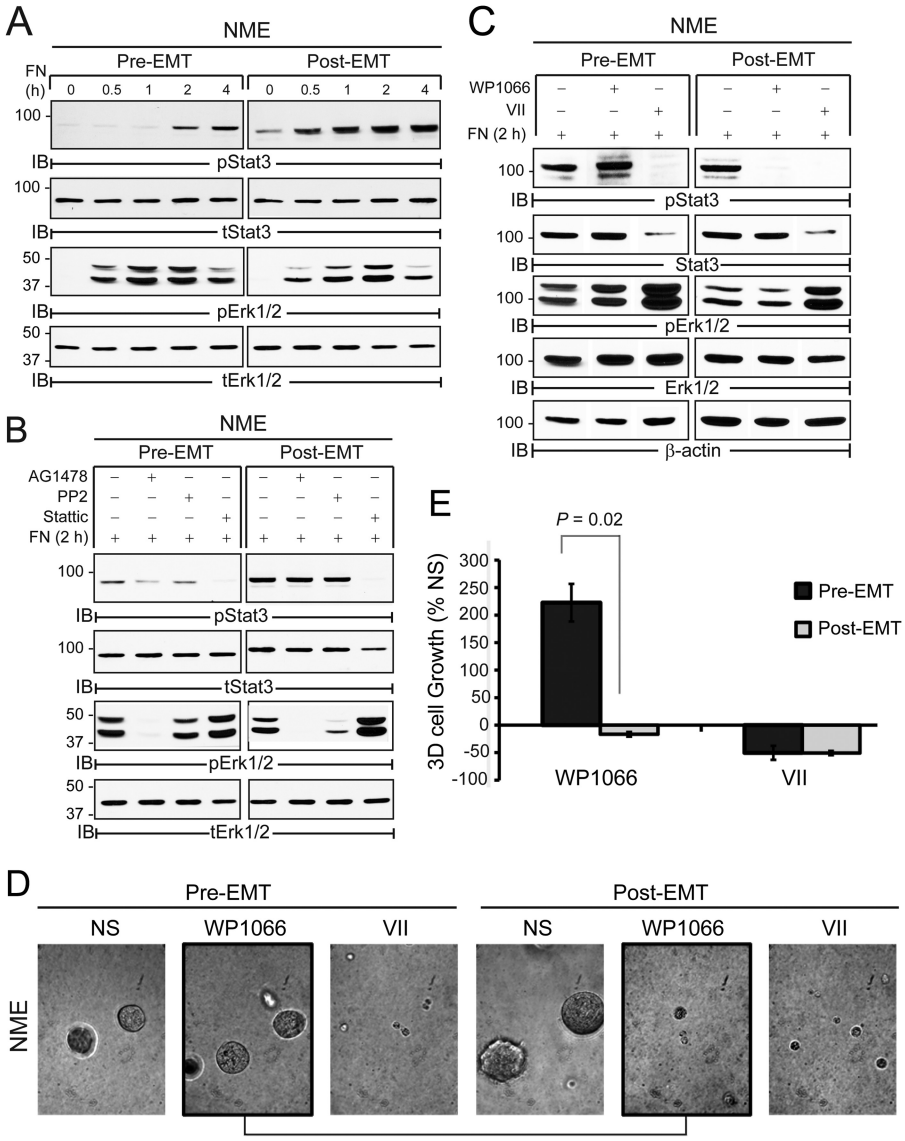

FIGURE 5. **EMT enhances FN:STAT3 signaling via a JAK2-dependent mechanism.** *A–C*, pre- and post-EMT NME cell populations (48 h pretreatment with TGF-β1) were seeded on FN up to 4 h (*A*), for 2 h following a 30-min pretreatment with SRC (10 μM PP2), EGFR (1 μM AG1478), or STAT3 (5 μM Stattic) inhibitors (*B*), or a 30-min pretreatment with the JAK2 (5 μM WP1066) or STAT3 (10 μM STAT3i VII) inhibitors prior to FN adhesion. *A–C*, equal aliquots were immunoblotted (*IB*) with phospho-specific and total protein antibodies as indicated. *D*, representative photomicrographs of pre- and post-EMT NME cell populations generated as in *panel A*, propagated in three-dimensional organotypic culture for 4 days the absence (*NS*) or presence of inhibitors to JAK2 (*WP1066*) or STAT3 (*VII*). *Bar*, ×400 magnification. *E*, three-dimensional cell growth in *D* quantified at 4 days post-plating by bioluminescence. Data are the mean of two independent experiments completed in triplicate (±S.E.).

subtype comprise ~10–20% of all BCs and are unique in their metastatic aggressiveness, increased rate of relapse, and poor overall prognosis (30, 48). Unfortunately, TNBC remains a diagnosis of exclusion defined only by their lack of estrogen receptor-α and progesterone receptor, and by their absence of human epidermal growth factor receptor 2 (HER2) amplification (48). As such, effective targeted molecular therapies against TNBC do not exist. Interestingly, TNBCs often exhibit elevated levels of EGFR expression, which is associated with decreased overall survival (9, 49). These findings suggest that administration of EGFR targeted therapies would alleviate TNBC disease progression, a supposition that has not been born out in clinical trials (50). Unlike other carcinomas where EGFR inhibitors are initially highly effective and resistance is "acquired" through tumor evolution, TNBCs are inherently resistant to EGFR inhibition. The mechanisms that drive this disconnect between the diagnostic and therapeutic efficacy of EGFR in BC remained poorly defined.

Our studies demonstrate the ability of FN to activate STAT3, thus contributing to aberrant cell growth within a physiologically relevant tumor microenvironment. These finding are supported by other recent studies demonstrating the ability of the ECM and cytoskeletal dynamics to directly initiate critical signaling pathways (51) and metastatic outgrowth (46). Furthermore, FN is a secreted matrix protein whose production is potently increased upon the induction of EMT. Therefore, our data establish a mechanism by which EMT may act in *trans* to activate STAT3 and influence the growth and/or metastasis of surrounding tumor cells. Moreover, disseminated tumor cells that have undergone EMT have the ability to establish a meta-

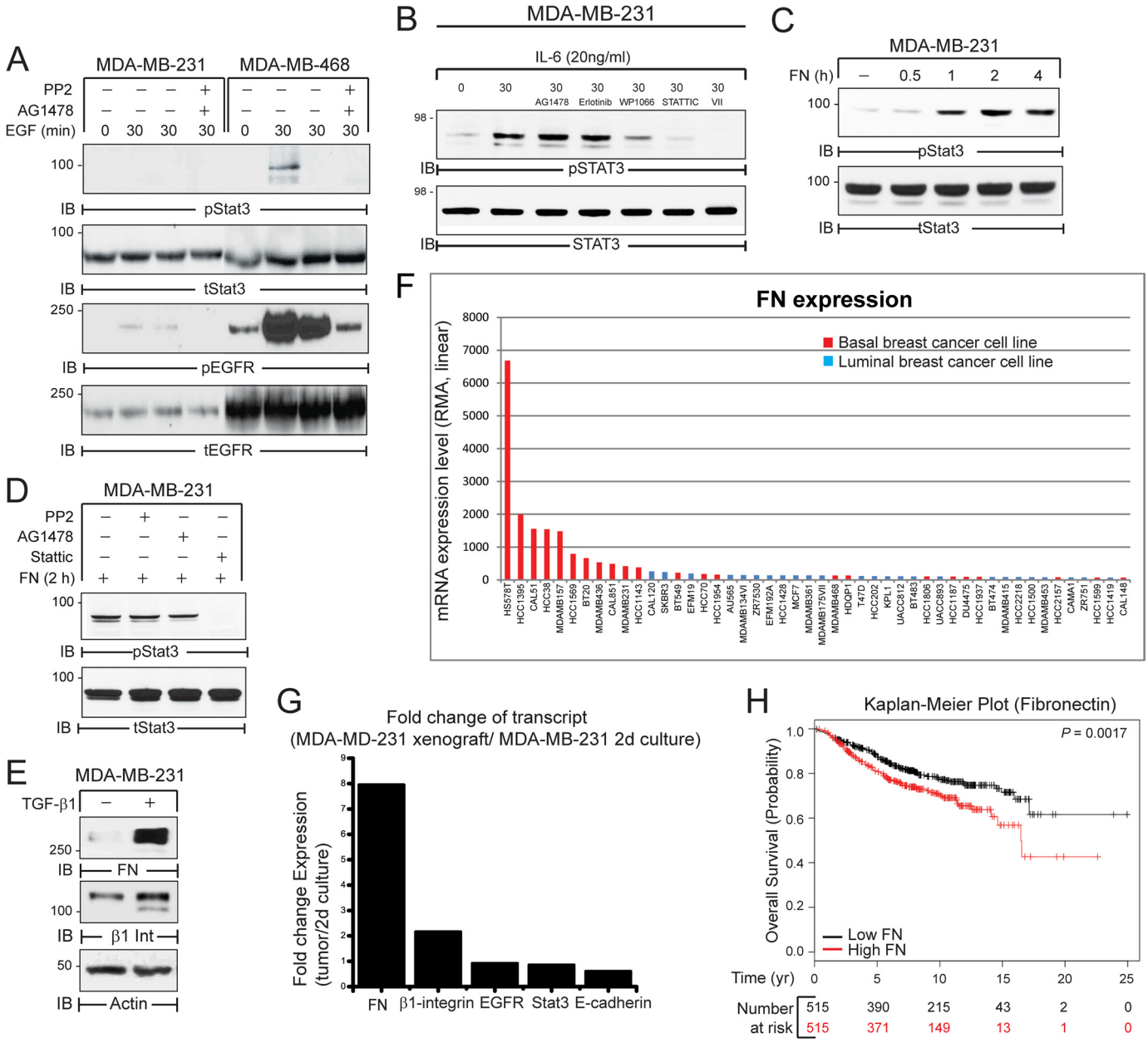

FIGURE 6. **FN activates STAT3 in human metastatic MDA-MB-231 cells.** *A*, MDA-MB-231 and MDA-MB-468 cells were serum deprived for 24 h and subsequently stimulated with EGF (50 ng/ml) for 30 min. *B*, MDA-MB-231 cells were serum deprived for 5 h and either left unstimulated (*NS*) or stimulated with IL-6 (20 ng/ml) for 30 min in the absence or presence of EGFR (1 μM Erlotinib; 1 μM AG1478), JAK2 (5 μM WP1066), and STAT3 (5 μM Stattic; 5 μM STAT3i VII) inhibitors for 30 min. *C* and *D*, MDA-MB-231 cells were left in suspension for 20 min or adhered to FN for up to 4 h (*B*), or adhered to FN for 2 h in the absence (−) or presence (+) of EGFR (1 μM AG1478), SRC (10 μM PP2), or STAT3 (10 μM Stattic) inhibitor (*C*). *A–D*, equal aliquots were analyzed by immunoblotting (*IB*) with the indicated phospho-specific and total protein antibodies. *E*, MDA-MB-231 cells were treated with TGF-β1 (5 ng/ml) for 48 h and analyzed by immunoblotting for expression of fibronectin (*FN*) and β1-integrin (*β1-Int*). Actin served as a loading control. *F*, $\log_2$ mRNA expression data for FN was collected for 58 human breast cancer cell lines housed in the Cancer Cell Line Encyclopedia and shown here on a linear scale following Robust Multi-Array Averaging (*RMA*). The indicated cell lines were annotated as basal or luminal based on review of the literature resulting in 48 classified cell lines. FN is expressed at higher levels in basal-like *versus* nonbasal-like counterparts. *G*, FN and β1 integrin expression are increased in MDA-MB-231 tumors compared with their *in vitro* cultured counterparts, whereas the expression of E-cadherin shows an inverse relationship between xenografts and cultured cells. *H*, Kaplan-Meier plot correlating FN expression and the probability of survival over a 25-year period in a cohort of 1027 BC patients split into low (*black*) and high (*red*) FN expression groups. The number of patients at risk in the low and high FN expression groups is indicated below the *x* axis.

static niche through EMT-induced autocrine FN production that supports STAT3 activation and metastatic outgrowth. Indeed, using a BC model in which transformation is initiated by EGFR overexpression, we show that EGF-mediated STAT3 signaling is actually diminished following the induction of EMT. Importantly, loss of growth factor responsiveness is associated with a concomitant increase in the ability of FN to stimulate this critical oncogenic pathway. Mechanistically, our data suggest that BCs switch away from SRC:EGFR-dependent STAT3 signaling to a compensatory pathway whereby β1 integrin receptors signal to PYK2/FAK during metastatic progression.

Of course the new FN:JAK2:STAT3 signaling pathway that we have elucidated in this study is only one facet of the unique

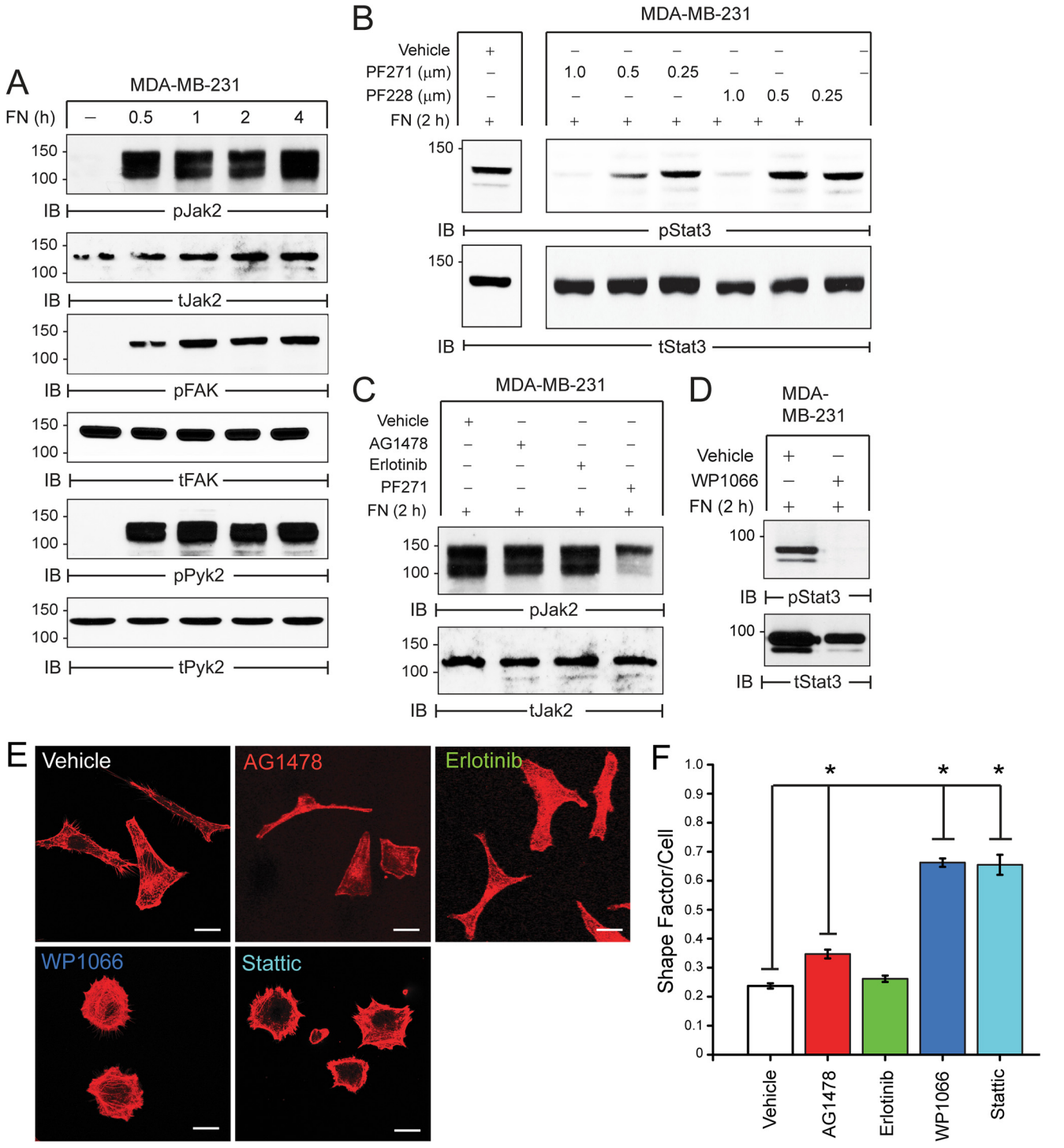

FIGURE 7. **A FN:FAK/PYK2:JAK2 pathway activates STAT3 in human metastatic MDA-MB-231 cells.** *A*, MDA-MB-231 cells were left in suspension (−) or adhered to FN for the indicated times. *B*, MDA-MB-231 cells were adhered to FN for 2 h in the presence of increasing concentrations of the FAK/PYK2 inhibitor PF572271 (*PF271*) or FAK-specific inhibitor PF573228 (*PF228*). *C*, MDA-MB-231 cells were adhered to FN in the absence (−) or presence (+) of EGFR (1 μM Erlotinib or 1 μM AG1478) or FAK/PYK2 (1 μM PF271) inhibitor. *D*, MDA-MB-231 cells were adhered to FN in the absence (−) or presence (+) of JAK2 inhibitor (1 μM WP1066). *A–D*, equal aliquots analyzed by immunoblot with the indicated phospho-specific and total protein antibodies. *E*, representative confocal images of MDA-MB-231 cells adhered to FN for 2 h in the presence of vehicle or EGFR (1 μM Erlotinib or 1 μM AG1478), JAK2 (3 μM WP1066), or STAT3 (3 μM Stattic) inhibitors. Cells were fixed and stained with phalloidin to visualize the actin cytoskeleton. *Size bars*, 5 μM. *F*, average shape factor/cell calculated from confocal images with values ranging from 0 to 1 for elongated to more rounded shapes, respectively (29). *, all p values < 0.05.

molecular phenotype of metastatic BC cells that is acquired through both genomic and nongenomic means. Other potentially critical factors that may be relevant in TNBC include the interplay between EGFR and insulin-like growth factor receptor signaling systems and production of cell surface effectors such as the subclass of heparin sulfate proteoglycans known as syndecans (52–56). Understanding how these different factors are integrated to drive metastatic progression will provide the

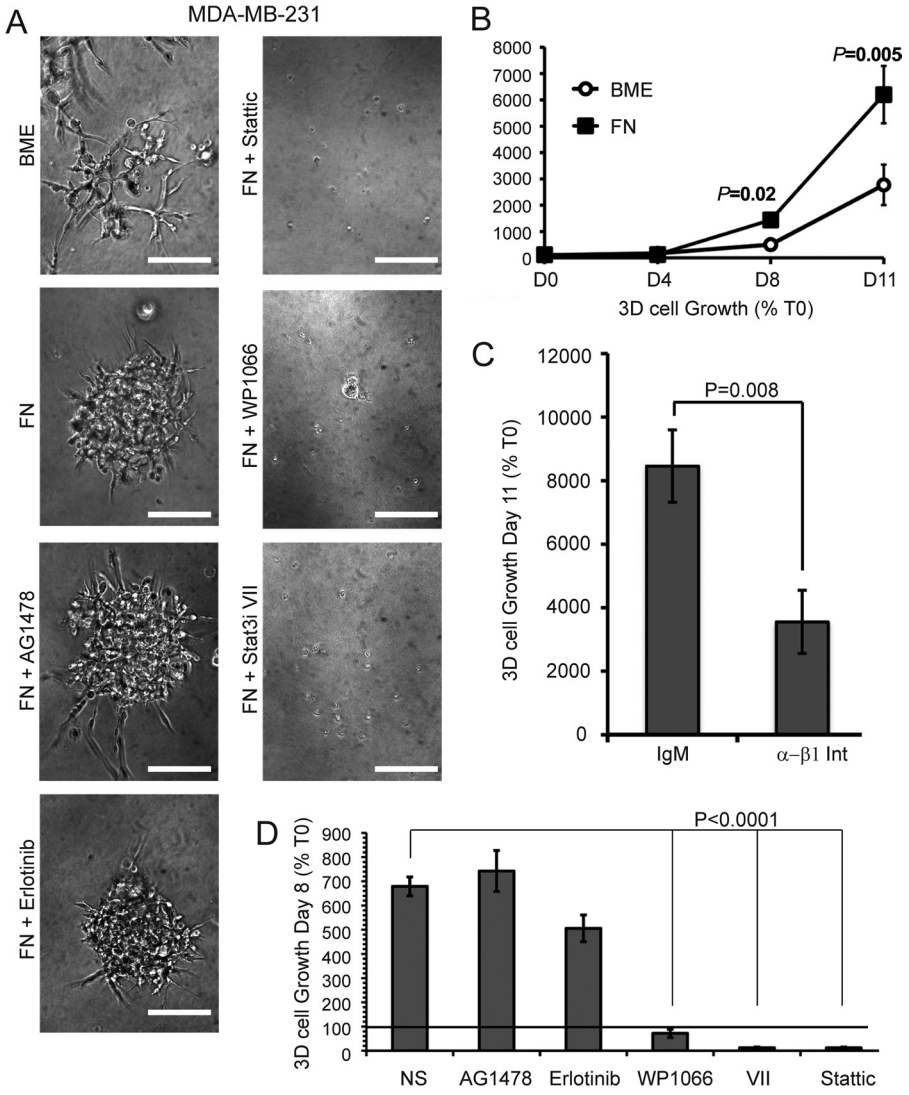

FIGURE 8. **FN:STAT3 signaling is required for 3D organotypic outgrowth of MDA-MB-231 cells.** *A*, representative photomicrographs of cells propagated in three-dimensional organotypic cultures for 11 days under control (basement membrane extract (*BME*)) or FN-supplemented conditions in the absence or presence of EGFR (1 μM Erlotinib or 1 μM AG1478), JAK2 (1 μM WP1066), or STAT3 (1 μM Stattic or 1 μM STAT3i VII) inhibitors. *Bars*, ×100 magnification. *B*, MDA-MB-231 cells were propagated in three-dimensional organotypic cultures with or without supplemental FN and longitudinal outgrowth was quantified by bioluminescence at the indicated time points. *C*, MDA-MB-231 cells were propagated under FN-supplemented three-dimensional conditions as in *panel B* in the absence (IgM) or presence of β1 integrin neutralizing antibody (α-β1-*Int*). Three-dimensional cellular outgrowth was quantified using a bioluminescence 11 days post-plating. *D*, three-dimensional cellular outgrowth of the MDA-MB-231 cells cultured in the absence (*NS*) or presence of EGFR (1 μM Erlotinib or 1 μM AG1478), JAK2 (1 μM WP1066), or STAT3 (1 μM STAT3 Inhibitor VII or 1 μM Stattic) inhibitors. Data in *panels B–D* are the mean ± S.E. of two independent experiments completed in triplicate.

basis for improved prognostic screening, guide individualized therapeutic choice, and further illuminate clinical resistance to EGFR-targeted therapies in TNBC patients.

Somewhat surprisingly, our data also appear to exclude a role for autocrine IL-6 because EMT programs fail to diminish the ability of NME cells to activate STAT3 in response to exogenous IL-6. Other investigators have shown that PYK2 forms a specific molecular complex with JAK2 responsible for activating selective JAK2 signaling responses (57, 58). Thus, it is reasonable to assume that FN-activated PYK2/FAK may fulfill a similar role in a JAK2:STAT3 signaling network, which is governed in an EMT-dependent manner. Underscoring the importance of this switch in upstream STAT3 signaling, we show that inhibition of JAK2 had no effect on BC organoid growth prior to induction of EMT. However, once these same cells have undergone EMT pharmacologic inhibition, JAK2 prevents BC outgrowth. These findings are quite remarkable as several recent studies suggest that the process of EMT is strongly linked to the acquisition of a stem-like and drug-resistant state (59). Indeed, our data clearly shows that BC cells acquire the ability to engage the matrix to facilitate cell signaling in the face of EGFR inhibition following EMT. Therefore, our JAK2 findings are quite unique in that they represent the first known example whereby EMT actually sensitizes BC cells to a targeted chemotherapy. These findings support the notion that JAK2 inhibition may be a viable option for treatment of late stage BC. Accordingly, inhibition of JAK2 is effective in abrogating three-dimensional growth of the human metastatic MDA-MB-231 cells that are resistant to inhibition of EGFR. Interestingly there are already phase II clinical trials addressing the effectiveness of JAK2 inhi-

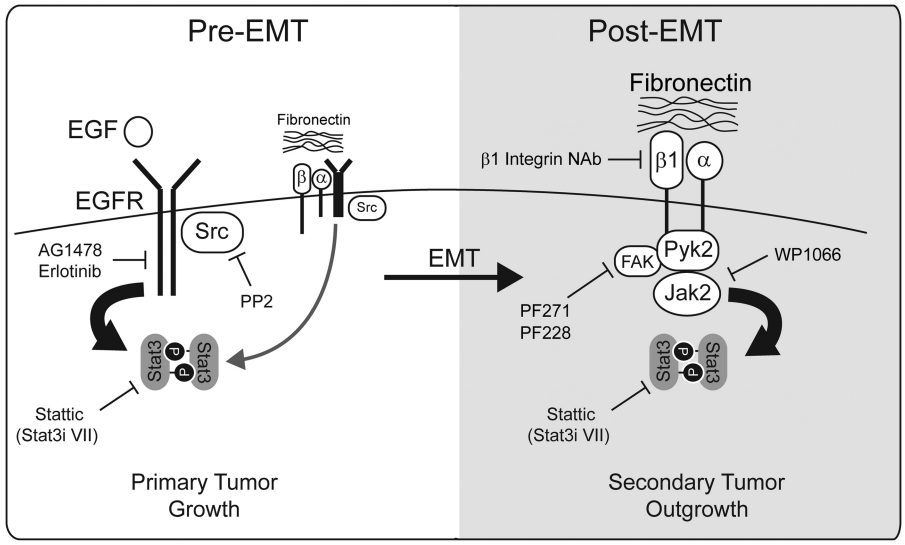

FIGURE 9. **STAT3 pathway switching is induced by EMT during breast cancer progression.** Early-stage BCs utilize SRC-dependent EGFR signaling to drive STAT3 activation and primary tumor growth. Although EGFR is capable of activating STAT3 downstream of FN engagement, the growth factor-stimulated pathway appears to be the prominent mode in pre-EMT cells. Late-stage BCs that have acquired EMT phenotypes utilize β1 integrin receptors to engage the ECM containing aberrant levels of FN thereby activating a FAK/PYK2:JAK2:STAT3 signaling cascade. This pathway may be clinically relevant at the metastatic tumor site and likely contributes to the resistance of BC to EGFR targeted therapies. Targets for pharmacological and immunological inhibitors used in this study are also highlighted.

bition in BC (60). Human MDA-MB-231 cells harbor activating Ras and BRAF mutations that are associated with constitutive MEK-Erk1/2 activation, which could account for EGFR-independent metastatic outgrowth (61). However, the effectiveness of β1 integrin, JAK2, and STAT3 inhibition in decreasing the outgrowth potential of these cells strongly implicates STAT3 as a critical signaling node mediating tumor outgrowth in FN-rich microenvironments even in cells harboring an alternative oncogenic pathway.

Collectively, our findings establish a novel form of EMT-mediated "pathway switching" that engages the tumor microenvironment to facilitate activation of critical signaling pathways. Our data illustrate a switch away from SRC-dependent EGFR:STAT3 signaling downstream of ligand stimulation or FN engagement as tumor cells undergo EMT. This is accompanied by a concomitant activation of an alternative pathway whereby FN activates β1 integrin receptors to elicit a FAK/PYK2:JAK2:STAT3 signaling pathway (Fig. 9). In addition to supporting the use of JAK2 inhibitors to specifically target post-EMT and metastatic BCs, our findings also indicate that development of novel strategies to prevent the switch in upstream STAT3 signaling may represent an important first step in re-sensitizing late-stage BCs to EGFR inhibitor therapies.

Acknowledgments—We thank Dr. Michael Simonson at Case Western Reserve University for advice on in silico data analysis. We also thank members of the Carlin and Schiemann laboratories for helpful comments and suggestions.

REFERENCES

1. Nelson, C. M., and Bissell, M. J. (2006) Of extracellular matrix, scaffolds, and signaling. Tissue architecture regulates development, homeostasis, and cancer. *Annu. Rev. Cell Dev. Biol.* **22,** 287–309
2. Barkan, D., Green, J. E., and Chambers, A. F. (2010) Extracellular matrix. A gatekeeper in the transition from dormancy to metastatic growth. *Eur. J. Cancer* **46,** 1181–1188
3. Cabodi, S., Moro, L., Bergatto, E., Boeri Erba, E., Di Stefano, P., Turco, E., Tarone, G., and Defilippi, P. (2004) Integrin regulation of epidermal growth factor (EGF) receptor and of EGF-dependent responses. *Biochem. Soc. Trans.* **32,** 438–442
4. Streuli, C. H., and Akhtar, N. (2009) Signal co-operation between integrins and other receptor systems. *Biochem. J.* **418,** 491–506
5. Balanis, N., Yoshigi, M., Wendt, M. K., Schiemann, W. P., and Carlin, C. R. (2011) β3 Integrin-EGF receptor cross-talk activates p190RhoGAP in mouse mammary gland epithelial cells. *Mol. Biol. Cell* **22,** 4288–4301
6. Galliher, A. J., Neil, J. R., and Schiemann, W. P. (2006) Role of transforming growth factor-β in cancer progression. *Future Oncol.* **2,** 743–763
7. Wendt, M. K., Smith, J. A., and Schiemann, W. P. (2010) Transforming growth factor-β-induced epithelial-mesenchymal transition facilitates epidermal growth factor-dependent breast cancer progression. *Oncogene* **29,** 6485–6498
8. Quintela, I., Corte, M. D., Allende, M. T., Vazquez, J., Rodríguez, J. C., Bongera, M., Lamelas, M., Gonzalez, L. O., Vega, A., García-Muñiz, J. L., Astudillo, A., and Vizoso, F. (2005) Expression and prognostic value of EGFR in invasive breast cancer. *Oncol. Rep.* **14,** 1655–1663
9. Ueno, N. T., and Zhang, D. (2011) Targeting EGFR in triple negative breast cancer. *J. Cancer* **2,** 324–328
10. Wyckoff, J., Wang, W., Lin, E. Y., Wang, Y., Pixley, F., Stanley, E. R., Graf, T., Pollard, J. W., Segall, J., and Condeelis, J. (2004) A paracrine loop between tumor cells and macrophages is required for tumor cell migration in mammary tumors. *Cancer Res.* **64,** 7022–7029
11. Flynn, J. F., Wong, C., and Wu, J. M. (2009) Anti-EGFR therapy. Mechanism and advances in clinical efficacy in breast cancer. *J. Oncol.* **2009,** 526963
12. Carey, L. A., Rugo, H. S., Marcom, P. K., Mayer, E. L., Esteva, F. J., Ma, C. X., Liu, M. C., Storniolo, A. M., Rimawi, M. F., Forero-Torres, A., Wolff, A. C., Hobday, T. J., Ivanova, A., Chiu, W. K., Ferraro, M., Burrows, E., Bernard, P. S., Hoadley, K. A., Perou, C. M., and Winer, E. P. (2012) TBCRC 001. Randomized phase II study of cetuximab in combination with carboplatin in stage IV triple-negative breast cancer. *J. Clin. Oncol.* **30,** 2615–2623
13. Wendt, M. K., Taylor, M. A., Schiemann, B. J., and Schiemann, W. P. (2011) Down-regulation of epithelial cadherin is required to initiate metastatic outgrowth of breast cancer. *Mol. Biol. Cell* **22,** 2423–2435
14. Ioachim, E., Charchanti, A., Briasoulis, E., Karavasilis, V., Tsanou, H., Ar-

vanitis, D. L., Agnantis, N. J., and Pavlidis, N. (2002) Immunohistochemical expression of extracellular matrix components tenascin, fibronectin, collagen type IV and laminin in breast cancer. Their prognostic value and role in tumour invasion and progression. *Eur. J. Cancer* **38,** 2362–2370
15. Ignotz, R. A., and Massagué, J. (1986) Transforming growth factor-β stimulates the expression of fibronectin and collagen and their incorporation into the extracellular matrix. *J. Biol. Chem.* **261,** 4337–4345
16. Marotta, L. L., Almendro, V., Marusyk, A., Shipitsin, M., Schemme, J., Walker, S. R., Bloushtain-Qimron, N., Kim, J. J., Choudhury, S. A., Maruyama, R., Wu, Z., Gönen, M., Mulvey, L. A., Bessarabova, M. O., Huh, S. J., Silver, S. J., Kim, S. Y., Park, S. Y., Lee, H. E., Anderson, K. S., Richardson, A. L., Nikolskaya, T., Nikolsky, Y., Liu, X. S., Root, D. E., Hahn, W. C., Frank, D. A., and Polyak, K. (2011) The JAK2/STAT3 signaling pathway is required for growth of CD44CD24 stem cell-like breast cancer cells in human tumors. *J. Clin. Invest.* **121,** 2723–2735
17. Idowu, M. O., Kmieciak, M., Dumur, C., Burton, R. S., Grimes, M. M., Powers, C. N., and Manjili, M. H. (2012) CD44(+)/CD24(-/low) cancer stem/progenitor cells are more abundant in triple-negative invasive breast carcinoma phenotype and are associated with poor outcome. *Hum. Pathol.* **43,** 364–373
18. Kamimura, D., Ishihara, K., and Hirano, T. (2003) IL-6 signal transduction and its physiological roles. The signal orchestration model. *Rev. Physiol. Biochem. Pharmacol.* **149,** 1–38
19. Fossey, S. L., Bear, M. D., Kisseberth, W. C., Pennell, M., and London, C. A. (2011) Oncostatin M promotes STAT3 activation, VEGF production, and invasion in osteosarcoma cell lines. *BMC Cancer* **11,** 125
20. Ho, H. H., and Ivashkiv, L. B. (2006) Role of STAT3 in type I interferon responses. Negative regulation of STAT1-dependent inflammatory gene activation. *J. Biol. Chem.* **281,** 14111–14118
21. Guren, T. K., Abrahamsen, H., Thoresen, G. H., Babaie, E., Berg, T., and Christoffersen, T. (1999) EGF-induced activation of Stat1, Stat3, and Stat5b is unrelated to the stimulation of DNA synthesis in cultured hepatocytes. *Biochem. Biophys. Res. Commun.* **258,** 565–571
22. Wendt, M. K., Schiemann, B. J., Parvani, J. G., Lee, Y. H., Kang, Y., and Schiemann, W. P. (2013) TGF-β stimulates Pyk2 expression as part of an epithelial-mesenchymal transition program required for metastatic outgrowth of breast cancer. *Oncogene* **32,** 2005–2015
23. Liao, H. J., and Carpenter, G. (2009) Cetuximab/C225-induced intracellular trafficking of epidermal growth factor receptor. *Cancer Res.* **69,** 6179–6183
24. Pruss, R. M., and Herschman, H. R. (1977) Variants of 3T3 cells lacking mitogenic response to epidermal growth factor. *Proc. Natl. Acad. Sci. U.S.A.* **74,** 3918–3921
25. Kostenko, O., Tsacoumangos, A., Crooks, D., Kil, S. J., and Carlin, C. (2006) Gab1 signaling is regulated by EGF receptor sorting in early endosomes. *Oncogene* **25,** 6604–6617
26. Wendt, M. K., and Schiemann, W. P. (2009) Therapeutic targeting of the focal adhesion complex prevents oncogenic TGF-β signaling and metastasis. *Breast Cancer Res.* **11,** R68
27. Crooks, D., Kil, S. J., McCaffery, J. M., and Carlin, C. (2000) E3–13.7 integral membrane proteins encoded by human adenoviruses alter epidermal growth factor receptor trafficking by interacting directly with receptors in early endosomes. *Mol. Biol. Cell* **11,** 3559–3572
28. Mendez, M. G., Kojima, S., and Goldman, R. D. (2010) Vimentin induces changes in cell shape, motility, and adhesion during the epithelial to mesenchymal transition. *FASEB J.* **24,** 1838–1851
29. Peris, L., Thery, M., Fauré, J., Saoudi, Y., Lafanechère, L., Chilton, J. K., Gordon-Weeks, P., Galjart, N., Bornens, M., Wordeman, L., Wehland, J., Andrieux, A., and Job, D. (2006) Tubulin tyrosination is a major factor affecting the recruitment of CAP-Gly proteins at microtubule plus ends. *J. Cell Biol.* **174,** 839–849
30. Lehmann, B. D., Bauer, J. A., Chen, X., Sanders, M. E., Chakravarthy, A. B., Shyr, Y., and Pietenpol, J. A. (2011) Identification of human triple-negative breast cancer subtypes and preclinical models for selection of targeted therapies. *J. Clin. Invest.* **121,** 2750–2767
31. Neve, R. M., Chin, K., Fridlyand, J., Yeh, J., Baehner, F. L., Fevr, T., Clark, L., Bayani, N., Coppe, J. P., Tong, F., Speed, T., Spellman, P. T., DeVries, S., Lapuk, A., Wang, N. J., Kuo, W. L., Stilwell, J. L., Pinkel, D., Albertson, D. G., Waldman, F. M., McCormick, F., Dickson, R. B., Johnson, M. D., Lippman, M., Ethier, S., Gazdar, A., and Gray, J. W. (2006) A collection of breast cancer cell lines for the study of functionally distinct cancer subtypes. *Cancer Cell* **10,** 515–527
32. Irizarry, R. A., Hobbs, B., Collin, F., Beazer-Barclay, Y. D., Antonellis, K. J., Scherf, U., and Speed, T. P. (2003) Exploration, normalization, and summaries of high density oligonucleotide array probe level data. *Biostatistics* **4,** 249–264
33. Győrffy, B., Lanczky, A., Eklund, A. C., Denkert, C., Budczies, J., Li, Q., and Szallasi, Z. (2010) An online survival analysis tool to rapidly assess the effect of 22,277 genes on breast cancer prognosis using microarray data of 1,809 patients. *Breast Cancer Res. Treat.* **123,** 725–731
34. Kil, S. J., Hobert, M., and Carlin, C. (1999) A leucine-based determinant in the epidermal growth factor receptor juxtamembrane domain is required for the efficient transport of ligand-receptor complexes to lysosomes. *J. Biol. Chem.* **274,** 3141–3150
35. Kil, S. J., and Carlin, C. (2000) EGF receptor residues Leu^{679}, Leu^{680} mediate selective sorting of ligand-receptor complexes in early endocytic compartments. *J. Cell Physiol.* **185,** 47–60
36. Coffer, P. J., and Kruijer, W. (1995) EGF receptor deletions define a region specifically mediating STAT transcription factor activation. *Biochem. Biophys. Res. Commun.* **210,** 74–81
37. Ng, D. C., Lin, B. H., Lim, C. P., Huang, G., Zhang, T., Poli, V., and Cao, X. (2006) Stat3 regulates microtubules by antagonizing the depolymerization activity of stathmin. *J. Cell Biol.* **172,** 245–257
38. McMurray, J. S. (2006) A new small-molecule Stat3 inhibitor. *Chem. Biol.* **13,** 1123–1124
39. Kenny, P. A., Lee, G. Y., Myers, C. A., Neve, R. M., Semeiks, J. R., Spellman, P. T., Lorenz, K., Lee, E. H., Barcellos-Hoff, M. H., Petersen, O. W., Gray, J. W., and Bissell, M. J. (2007) The morphologies of breast cancer cell lines in three-dimensional assays correlate with their profiles of gene expression. *Mol. Oncol.* **1,** 84–96
40. Dawson, P. J., Wolman, S. R., Tait, L., Heppner, G. H., and Miller, F. R. (1996) MCF10AT. A model for the evolution of cancer from proliferative breast disease. *Am. J. Pathol.* **148,** 313–319
41. Cailleau, R., Olivé, M., and Cruciger, Q. (1978) Long-term human breast carcinoma cell lines of metastatic origin. Preliminary characterization. *In Vitro* **14,** 911–915
42. Lo, H. W., Hsu, S. C., Xia, W., Cao, X., Shih, J. Y., Wei, Y., Abbruzzese, J. L., Hortobagyi, G. N., and Hung, M. C. (2007) Epidermal growth factor receptor cooperates with signal transducer and activator of transcription 3 to induce epithelial-mesenchymal transition in cancer cells via up-regulation of TWIST gene expression. *Cancer Res.* **67,** 9066–9076
43. Filmus, J., Trent, J. M., Pollak, M. N., and Buick, R. N. (1987) Epidermal growth factor receptor gene-amplified MDA-468 breast cancer cell line and its nonamplified variants. *Mol. Cell Biol.* **7,** 251–257
44. Padua, D., Zhang, X. H., Wang, Q., Nadal, C., Gerald, W. L., Gomis, R. R., and Massagué, J. (2008) TGFβ primes breast tumors for lung metastasis seeding through angiopoietin-like 4. *Cell* **133,** 66–77
45. Hynes, R. O., Lively, J. C., McCarty, J. H., Taverna, D., Francis, S. E., Hodivala-Dilke, K., and Xiao, Q. (2002) The diverse roles of integrins and their ligands in angiogenesis. *Cold Spring Harb. Symp. Quant. Biol.* **67,** 143–153
46. Barkan, D., Kleinman, H., Simmons, J. L., Asmussen, H., Kamaraju, A. K., Hoenorhoff, M. J., Liu, Z. Y., Costes, S. V., Cho, E. H., Lockett, S., Khanna, C., Chambers, A. F., and Green, J. E. (2008) Inhibition of metastatic outgrowth from single dormant tumor cells by targeting the cytoskeleton. *Cancer Res.* **68,** 6241–6250
47. Shibue, T., and Weinberg, R. A. (2009) Integrin β1-focal adhesion kinase signaling directs the proliferation of metastatic cancer cells disseminated in the lungs. *Proc. Natl. Acad. Sci. U.S.A.* **106,** 10290–10295
48. Dent, R., Trudeau, M., Pritchard, K. I., Hanna, W. M., Kahn, H. K., Sawka, C. A., Lickley, L. A., Rawlinson, E., Sun, P., and Narod, S. A. (2007) Triple-negative breast cancer. Clinical features and patterns of recurrence. *Clin. Cancer Res.* **13,** 4429–4434
49. Tischkowitz, M., Brunet, J. S., Bégin, L. R., Huntsman, D. G., Cheang, M. C., Akslen, L. A., Nielsen, T. O., and Foulkes, W. D. (2007) Use of immunohistochemical markers can refine prognosis in triple negative

breast cancer. *BMC Cancer* **7,** 134
50. Dickler, M. N., Rugo, H. S., Eberle, C. A., Brogi, E., Caravelli, J. F., Panageas, K. S., Boyd, J., Yeh, B., Lake, D. E., Dang, C. T., Gilewski, T. A., Bromberg, J. F., Seidman, A. D., D'Andrea, G. M., Moasser, M. M., Melisko, M., Park, J. W., Dancey, J., Norton, L., and Hudis, C. A. (2008) A phase II trial of erlotinib in combination with bevacizumab in patients with metastatic breast cancer. *Clin. Cancer Res.* **14,** 7878–7883
51. Dupont, S., Morsut, L., Aragona, M., Enzo, E., Giulitti, S., Cordenonsi, M., Zanconato, F., Le Digabel, J., Forcato, M., Bicciato, S., Elvassore, N., and Piccolo, S. (2011) Role of YAP/TAZ in mechanotransduction. *Nature* **474,** 179–183
52. Tsonis, A. I., Afratis, N., Gialeli, C., Ellina, M. I., Piperigkou, Z., Skandalis, S. S., Theocharis, A. D., Tzanakakis, G. N., and Karamanos, N. K. (2013) Evaluation of the coordinated actions of estrogen receptors with epidermal growth factor receptor and insulin-like growth factor receptor in the expression of cell surface heparan sulfate proteoglycans and cell motility in breast cancer cells. *FEBS J.* **280,** 2248–2259
53. Song, R. X., Chen, Y., Zhang, Z., Bao, Y., Yue, W., Wang, J. P., Fan, P., and Santen, R. J. (2010) Estrogen utilization of IGF-1-R and EGF-R to signal in breast cancer cells. *J. Steroid Biochem. Mol. Biol.* **118,** 219–230
54. Ibrahim, S. A., Yip, G. W., Stock, C., Pan, J. W., Neubauer, C., Poeter, M., Pupjalis, D., Koo, C. Y., Kelsch, R., Schüle, R., Rescher, U., Kiesel, L., and Götte, M. (2012) Targeting of syndecan-1 by microRNA miR-10b promotes breast cancer cell motility and invasiveness via a Rho-GTPase- and E-cadherin-dependent mechanism. *Int. J. Cancer* **131,** E884–896
55. Rousseau, C., Ruellan, A. L., Bernardeau, K., Kraeber-Bodéré, F., Gouard, S., Loussouarn, D., Saï-Maurel, C., Faivre-Chauvet, A., Wijdenes, J., Barbet, J., Gaschet, J., Chérel, M., and Davodeau, F. (2011) Syndecan-1 antigen, a promising new target for triple-negative breast cancer immuno-PET and radioimmunotherapy. A preclinical study on MDA-MB-468 xenograft tumors. *EJNMMI Res.* **1,** 20
56. Qian, X. L., Li, Y. Q., Yu, B., Gu, F., Liu, F. F., Li, W. D., Zhang, X. M., and Fu, L. (2013) Syndecan Binding Protein (SDCBP) is overexpressed in estrogen receptor negative breast cancers, and is a potential promoter for tumor proliferation. *PLoS One* **8,** e60046
57. Zhu, T., Goh, E. L., and Lobie, P. E. (1998) Growth hormone stimulates the tyrosine phosphorylation and association of p125 focal adhesion kinase (FAK) with JAK2. Fak is not required for STAT-mediated transcription. *J. Biol. Chem.* **273,** 10682–10689
58. Takaoka, A., Tanaka, N., Mitani, Y., Miyazaki, T., Fujii, H., Sato, M., Kovarik, P., Decker, T., Schlessinger, J., and Taniguchi, T. (1999) Protein tyrosine kinase Pyk2 mediates the Jak-dependent activation of MAPK and Stat1 in IFN-γ, but not IFN-α, signaling. *EMBO J.* **18,** 2480–2488
59. Singh, A., and Settleman, J. (2010) EMT, cancer stem cells and drug resistance. An emerging axis of evil in the war on cancer. *Oncogene* **29,** 4741–4751
60. Dana Farber Cancer Institute (March 28, 2012) Ruxolitinib in patients with breast cancer. National Library of Medicine (US), www.clinicaltrials.gov/show/NCT01562873, NLM identifier: NCT0004451
61. Wilhelm, S. M., Adnane, L., Newell, P., Villanueva, A., Llovet, J. M., and Lynch, M. (2008) Preclinical overview of sorafenib, a multikinase inhibitor that targets both Raf and VEGF and PDGF receptor tyrosine kinase signaling. *Mol. Cancer Ther.* **7,** 3129–3140